

# Large deviations in stochastic dynamics over graphs through Matrix Product Belief Propagation

Stefano Crotti<sup>1,\*</sup> and Alfredo Braunstein<sup>1,2,3</sup>

<sup>1</sup>Politecnico di Torino, Corso duca degli Abruzzi 24, 10124 Torino

<sup>2</sup>Italian Institute for Genomic Medicine, IRCCS Candiolo, SP-142, I-10060, Candiolo (TO), Italy

<sup>3</sup>INFN, Sezione di Torino, Torino, Italy

Stochastic processes on graphs can describe a great variety of phenomena ranging from vehicular traffic to neural activity and epidemic spreading. While many existing methods can accurately describe typical realizations of such processes, computing properties of extremely rare events is generally a hard task. In particular, good approximations are lacking for models with recurrent dynamics, in which variables can return to a previously visited state. Recently, a scheme based on the cavity method with messages parametrized by matrix product states [T. Barthel, C. De Bacco, and S. Franz, Physical Review E 97, 010104 (2018)] has been shown to work well for typical trajectories. In this work, we build on this approach in two directions: first, we show how, using a general formulation of the belief propagation equations instead of the dynamical cavity method, it can be applied to Markov processes biased by arbitrary reweighting factors that concentrate most of the probability mass on rare events. Second, we introduce an efficient scheme to reduce the computational cost of a single node update from exponential to polynomial in the node degree, allowing to apply the method to graphs of large connectivity. Two applications are considered. First, we compute individual infection probabilities from sparse observations within the SIRS epidemic model (the risk assessment problem). Second, we compute typical observables and large deviations of Glauber dynamics on several Ising models, including a random field ferromagnet and a spin glass.

## I. INTRODUCTION

The problem of computing observables and marginal probabilities on a complex Markov process on large networks has been addressed extensively in the literature. While Monte-Carlo procedures can be often effective to compute averages approximately, they suffer from two separate issues: large relative sampling errors when computing averages that cancel out at the first order and they are limited to sampling “typical” events, as nontypical ones require an exponential number of samples. To address the first issue, many analytical solutions, mainly based on mean-field methods, have been devised [1–7]. A solution that is exact on acyclic graphs is Dynamic Cavity (DC) [8]. DC on general processes suffers from one main drawback, the fact that one must be able to represent the joint distribution of a single variable trajectory and a feedback field, and with some exceptions, the space of these trajectories is exponentially large (in the time horizon), and thus the approach becomes impractical. One of these exceptions is on “non-recurrent” models, i.e. models in which each variable can only progress sequentially through a finite set of  $k$  states, never going back to a previous state. In these cases the set of trajectories is polynomial in the time horizon (as an example with  $q = 3$ , a trajectory  $(1, 1, 2, 2, 2, 2, 3, 3)$  on epochs  $t = 0, \dots, 7$  can be represented by the integer tuple  $(2, 6)$  of epochs on which the variable effectively progresses to the next state in the sequence). Examples of non-recurrent models are the SI, SIR, SEIR compartmental models in computational epidemics, in which an

individual can only transition from Susceptible to Exposed, from Exposed to Infective and from Infective to Recovered. While the use of non-recurrent models is pervasive, oftentimes a more realistic description demands that re-infections be taken into account. In such cases, “recurrent” models such as the SIS and SIRS are employed. Additionally, important processes in statistical physics such as Glauber dynamics belong to the class of models with recurrence.

In a brilliant work by Barthel et al. [9, 10], a DC variant was proposed that exploits the Matrix Product State representation (MPS) to parametrize site trajectories and applied it to the Glauber dynamics on a Random Regular (RR) graph with degree 3. While these results are promising, the scheme suffers from two major limitations: first, it is computationally expensive (the update on a node of degree  $z$  is of the order of  $M^{2z-1}$  [10] where  $M$  is the matrix dimension), making it impractical even for moderately large Erdos-Renyi (ER) random graphs, in which some large-degree vertices are surely present. Second, the scheme is devised to analyze a “free” dynamics without any sort of reweighting, which as we will see is necessary to study atypical trajectories. Matrix Product States, also known as Tensor Trains, are not new in physics and other areas of science, as they have been successfully applied both in many-body quantum systems [11–13], out-of-equilibrium statistical physics [14, 15], machine learning [16, 17] and more.

We propose an alternative approach, dubbed Matrix Product Belief Propagation (MPBP), based on the Pair Trajectory Belief Propagation formulation which was first introduced in [18]. It is closely related to DC but allows naturally to include non-negative reweighting terms on stochastic trajectories, thus allowing to study large

\* stefano.crotti@polito.it

deviations of the system. In practical terms, MPBP consist on a fixed point equation that is solved by iteration, whereas DC is solved sequentially in time, with a number of steps which is equal to the number of epochs of the dynamics. The latter approach is inherently limited to free dynamics: building trajectories sequentially in time makes it impossible to account for the effect of reweighting terms relative to future epochs.

The Julia code used to implement the method and produce the data presented in this work is publicly accessible at [19].

We describe in the following the models under consideration. Given a graph  $G = (V, E)$  with  $V = \{1, \dots, N\}$ , consider a joint distribution over a set of discrete variables  $\mathbf{x} = \{x_1, \dots, x_N\}$  throughout  $T$  successive epochs of the form

$$p(\bar{\mathbf{x}}) = \frac{1}{Z} \prod_{t=0}^{T-1} \prod_{i=1}^N f_i^{t+1}(x_i^{t+1}, \mathbf{x}_{\partial i}^t, x_i^t). \quad (1)$$

We use bold letters to indicate multiple variable indices  $\mathbf{x}_A \equiv \{x_j\}_{j \in A}$  and overbars for multiple times indices  $\bar{\mathbf{x}} \equiv \{x^t\}_{t=0:T}$ . Moreover, we indicate by  $\partial i = \{j : (ij) \in E\}$  the set of neighbors of index  $i$ .

The form (1) includes (but notably is more general than) reweighted Markov dynamics  $f_i^{t+1}(x_i^{t+1}, \mathbf{x}_{\partial i}^t, x_i^t) = w(x_i^0)^{\delta(t,0)} w(x_i^{t+1} | \mathbf{x}_{\partial i}^t, x_i^t) \phi_i^t(x_i^t)$  with stochastic transitions  $w$  and reweighting factors  $\phi$

$$p(\bar{\mathbf{x}}) = \frac{1}{Z} \prod_{i=1}^N w(x_i^0) \prod_{t=0}^{T-1} w(x_i^{t+1} | \mathbf{x}_{\partial i}^t, x_i^t) \phi_i^t(x_i^t). \quad (2)$$

Note that  $Z = 1$  in the absence of reweighting factors  $\phi$ . Two types of reweighted dynamics of the form (2) will be used as running examples throughout this work. The first is Bayesian inference on a process of epidemic spreading. The posterior probability of the epidemic trajectory  $\bar{\mathbf{x}}$  given some independent observations  $\{O_i^t\}$  on the system is given by

$$p(\bar{\mathbf{x}}|O) = \frac{1}{p(O)} p(\bar{\mathbf{x}}) p(O|\bar{\mathbf{x}}) \quad (3)$$

$$= \frac{1}{Z} \prod_{i=1}^N w(x_i^0) \prod_{t=0}^{T-1} w(x_i^{t+1} | \mathbf{x}_{\partial i}^t, x_i^t) p(O_i^t | x_i^t) \quad (4)$$

where the specific form of the  $w$ 's depends on the chosen epidemiological model. The simplest among the recurrent epidemiological models is the Susceptible-Infectious-Susceptible (SIS), where each individual starts with a probability  $\gamma_i$  of being infectious at time zero. Then at each time step a susceptible node  $i$  can be infected by each of its infectious neighbors  $j \in \partial i$  with probability  $\lambda_{ji}$ , and an Infectious node can recover with probability  $\rho_i$ . Observation terms  $p(O_i^t | x_i^t)$  are naturally used to

model medical tests:  $O_i^t$  is the outcome of a test performed on individual  $i$  at time  $t$ . This formalism allows to incorporate information about the degree of accuracy of tests.

The second example is parallel Glauber dynamics for an Ising model at inverse temperature  $\beta$  with couplings  $\{J_{ij}\}$  and external fields  $\{h_i\}$ . Besides being one of the paradigmatic models in theoretical non-equilibrium statistical physics, Glauber dynamics is employed in the study neural activity [20, 21]. It is defined by transitions

$$\tilde{w}(\sigma_i^{t+1} | \sigma_{\partial i}^t) = \frac{e^{\beta \sigma_i^{t+1} (\sum_{j \in \partial i} J_{ij} \sigma_j^t + h_i)}}{2 \cosh [\beta (\sum_{j \in \partial i} J_{ij} \sigma_j^t + h_i)]}. \quad (5)$$

Additionally, we allow to return to the same state with some probability  $p_0$ . The transition thus becomes

$$w(\sigma_i^{t+1} | \sigma_{\partial i}^t, \sigma_i^t) = (1 - p_0) \tilde{w}(\sigma_i^{t+1} | \sigma_{\partial i}^t) + p_0 \delta(\sigma_i^{t+1}, \sigma_i^t). \quad (6)$$

Such dynamics can be “tilted” with e.g. a term  $\prod_i \phi_i^T(\sigma_i^T) = \prod_i e^{h \sigma_i^T}$  in order to study atypical trajectories. Note that other models studied in physics such as Bootstrap Percolation can be remapped into Glauber dynamics [22].

## II. METHOD DESCRIPTION

### A. Related work

*a. Mean-field methods* We briefly review the main features of existing approaches based on the cavity method. Dynamic Message Passing (DMP) [2, 23, 24] and the Cavity Master Equation [6, 7] are simple and fast approximate methods that were originally formulated on continuous time as ODEs for a vector of single-edge quantities (such as cavity magnetizations). Both methods are exact on acyclic graphs on non-recurrent models (such as SI or SIR), but only approximate on non-non-recurrent ones, and do not allow for atypical trajectories.  $n$ -step Dynamic Message Passing [3] makes an  $n$ -Markov *ansatz* on messages, exploring mainly  $n = 1$ ; its features are essentially those of DMP, with the difference that it applies to discrete time evolution and describes explicitly interactions at distance  $n$  in time. Different flavors of the cluster variational method [5, 25] approximate the dynamics by treating exactly correlations between variables that are close either in time or space. Large deviations have been studied in [26] using a perturbation theory in the particular case of Glauber dynamics on a chain. Table I summarizes the features of the methods mentioned above. We take into consideration: ability to deal with reweighted dynamics, ability to deal with recurrent models, possibility of extension to infinite graphs (thermodynamic limit) and to compute autocorrelations at arbitrary (time) distance.

	reweighting	Recurrent models	Autocorrelations
BP for non-recurrent models [18]	Y	N	Y
IBMF [1], DMP [2, 3, 24], CME [6]	N	Y	N
Dynamic Cluster Variational [5]	*	Y	Only two-times
Matrix Product Dynamic Cavity [9]	N	Y	Y
Matrix Product Belief Propagation	Y	Y	Y

Table I. Features of existing analytical methods for the description of stochastic dynamics on graphs, Y for yes, N for no. The asterisks mean that the method could in principle be extended to include the considered feature although this has not, to the best of our knowledge, been done in the literature. IBMF stands for Individual-Based Mean Field, DMP for Dynamic Message Passing, CME for Cavity Master Equation. We did not include the perturbative approach [26] because it focuses on a very particular setting.

*b. Monte Carlo* Throughout this work, the performance of algorithms is compared with Monte Carlo simulations. To estimate observables in a reweighted dynamics of the form (2) we employ a weighted sampling technique (see e.g. [27]): the posterior average of an observable  $f$  is approximated by

$$\hat{f} = \frac{\sum_{\mu=1}^M \prod_{i,t} \phi_i^t((x_i^t)^{(\mu)}) f(\bar{\mathbf{x}}^{(\mu)})}{\sum_{\mu=1}^M \prod_{i,t} \phi_i^t((x_i^t)^{(\mu)})} \quad (7)$$

where  $\{\bar{\mathbf{x}}^{(\mu)}\}_{\mu}$  are  $M$  independent samples drawn from the prior  $\prod_{i=1}^N w(x_i^0) \prod_{t=0}^{T-1} w(x_i^{t+1} | \mathbf{x}_{\partial i}^t, x_i^t)$ . Such strategy, however, turns out to be computationally prohibitive whenever the reweighting terms  $\phi$  put most of the probability mass on atypical trajectories, which are (exponentially) unlikely to ever be sampled.

## B. Matrix Product Belief Propagation

The dynamic version of Belief Propagation (BP) is relatively similar to Dynamic Cavity, with the difference that here the dynamical problem is first mapped into a model of interaction of site trajectories, at which point the regular BP formalism applies straightforwardly. As a preliminary step, one builds the factor graph associated with the joint distribution of the dynamics (1), where the variable at node  $i$  is the trajectory  $\bar{x}_i$ . The factor graph will present many small loops, therefore we choose to work on the so-called dual factor graph where variables are pair of trajectories  $(\bar{x}_i, \bar{x}_j)$  living on the edges of the original graph. For more details about this step we refer the reader to [18, fig. 3, eqns 8,9]. The Belief Propagation (BP) equations on the dual factor graph read

$$m_{i \rightarrow j}(\bar{x}_i, \bar{x}_j) \propto \sum_{\bar{x}_{\partial i \setminus j}} \prod_{t=0}^{T-1} f_i^{t+1}(x_i^{t+1}, \mathbf{x}_{\partial i}^t, x_i^t) \times \prod_{k \in \partial i \setminus j} m_{k \rightarrow i}(\bar{x}_k, \bar{x}_i) \quad (8)$$

and single-variable marginals, “beliefs”, are given by

$$b_i(\bar{x}_i) \propto \sum_{\bar{x}_{\partial i}} \prod_{t=0}^{T-1} f_i^{t+1}(x_i^{t+1}, \mathbf{x}_{\partial i}^t, x_i^t) \times \prod_{k \in \partial i} m_{k \rightarrow i}(\bar{x}_k, \bar{x}_i). \quad (9)$$

Similarly to [9], we parametrize messages  $m_{i \rightarrow j}$  in terms of matrix products

$$m_{i \rightarrow j}(\bar{x}_i, \bar{x}_j) \propto \prod_{t=0}^T A_{i \rightarrow j}^t(x_i^t, x_j^t) \quad (10)$$

where, for a specific choice of  $(x_i^t, x_j^t)$ ,  $A_{i \rightarrow j}^t(x_i^t, x_j^t)$  is a real-valued matrix. We set  $A^0$  to have one row and  $A^T$  to have one column, so that the whole product gives a scalar. Plugging the *ansatz* (10) into the RHS of (8) gives

$$m_{i \rightarrow j}(\bar{x}_i, \bar{x}_j) \propto \prod_{t=0}^T B_{i \rightarrow j}^t(x_i^{t+1}, x_i^t, x_j^t) \quad (11)$$

with

$$B_{i \rightarrow j}^t(x_i^{t+1}, x_i^t, x_j^t) = \sum_{\{x_k^t\}_{k \in \partial i \setminus j}} f_i^{t+1}(x_i^{t+1}, \mathbf{x}_{\partial i}^t, x_i^t) \times \left[ \bigotimes_{k \in \partial i \setminus j} A_{i \rightarrow j}^t(x_i^t, x_j^t) \right]. \quad (12)$$

Two steps are missing in order to close the BP equations under a matrix product *ansatz* (we note that this

technique is already present e.g. in [9]). First, matrices must be recast into the form (10). Second, if incoming  $A$  matrices have size  $M$ ,  $B$  matrices will have size  $M^{|\partial i| - 1}$  and thus will keep growing indefinitely throughout the iterations. Both issues are solved by means of two successive sweeps of Singular Value Decompositions (SVD). SVD decomposes a real-valued matrix  $A$  as  $A_{ij} = \sum_{k,l=1}^M U_{ik} \Lambda_{kl} V_{jl}$  where  $\Lambda_{kl} = \lambda_k \delta_{k,l}$  is the diagonal matrix of singular values  $\lambda_1 \geq \lambda_2 \geq \dots \geq \lambda_M \geq 0$  and  $U^\dagger U = VV^\dagger = \mathbb{1}$  (we use the dagger symbol for matrix transpose to avoid confusion with the time labels  $t, T$ , but all matrices are real-valued). By retaining only the largest  $M'$  singular values and setting the others to zero, one can approximate  $A$  with  $\tilde{A}_{ij} := \sum_{k=1}^{M'} U_{ik} \lambda_k V_{jk}$  making an error  $\|A - \tilde{A}\|_F^2 = \sum_{ij} (A_{ij} - \tilde{A}_{ij})^2 = \sum_{k=M'+1}^M \lambda_k^2$ . As a result, both  $U$  and  $V$  are smaller in size.

The first sweep of SVDs is done from left to right  $t = 0, 1, 2, \dots, T-1$

$$\begin{aligned} B_{i \rightarrow j}^t(x_i^{t+1}, x_i^t, x_j^t) &\stackrel{\text{SVD}}{=} C_{i \rightarrow j}^t(x_i^t, x_j^t) \Lambda V^\dagger(x_i^{t+1}) \\ B_{i \rightarrow j}^{t+1}(x_i^{t+2}, x_i^{t+1}, x_j^{t+1}) &\leftarrow \Lambda V^\dagger(x_i^{t+1}) B_{i \rightarrow j}^{t+1}(x_i^{t+2}, x_i^{t+1}, x_j^{t+1}) \end{aligned} \quad (13)$$

where the decomposition in the first line is performed by incorporating  $x_i^t, x_j^t$  as row indices and  $x_i^{t+1}$  as column index (see the appendix for more details). At the end of this first sweep, the message looks like

$$m_{i \rightarrow j}(\bar{x}_i, \bar{x}_j) = \prod_{t=0}^T C_{i \rightarrow j}^t(x_i^t, x_j^t) \quad (14)$$

where, thanks to the properties of the SVD, it holds that

$$\sum_{x_i^t x_j^t} [C_{i \rightarrow j}^t(x_i^t, x_j^t)]^\dagger C_{i \rightarrow j}^t(x_i^t, x_j^t) = \mathbb{1}. \quad (15)$$

At this point the form (10) is recovered: the BP equations are closed under a matrix product *ansatz*. All is left is to do is perform a second sweep of SVD, this time discarding the smallest singular values to obtain matrices of reduced size. Going right to left  $t = T, T-1, \dots, 1$ , incorporating  $(x_i^t, x_j^t)$  as column indices:

$$\begin{aligned} C_{i \rightarrow j}^t(x_i^t, x_j^t) &\stackrel{\text{SVD,trunc}}{=} U \Lambda A_{i \rightarrow j}^t(x_i^t, x_j^t) \\ C_{i \rightarrow j}^{t-1}(x_i^{t-1}, x_j^{t-1}) &\leftarrow C_{i \rightarrow j}^{t-1}(x_i^{t+1}, x_j^{t+1}) U \Lambda \end{aligned} \quad (16)$$

The errors made during the truncations are controlled: consider a generic step  $t$  in the sweep from right to left. We are in the following situation:

$$C^0 \cdots C^t A^{t+1} \cdots A^T \quad (17)$$

with  $C^0 \cdots C^{t-1}$  left-orthogonal ( $C^\dagger C = \mathbb{1}$ ) and  $A^{t+1} \cdots A^T$  right-orthogonal ( $AA^\dagger = \mathbb{1}$ ).  $C^t$  is neither.

The error in replacing  $C^t$  by  $\tilde{C}^t$  which retains only  $M'$  of the  $M$  singular values is

$$\begin{aligned} \|C^0 \cdots C^t A^{t+1} \cdots A^T - C^0 \cdots \tilde{C}^t A^{t+1} \cdots A^T\|_F^2 \\ = \|C^t - \tilde{C}^t\|_F^2 = \sum_{k=M'+1}^M \lambda_k^2 \end{aligned} \quad (18)$$

where the first equality holds thanks to the orthonormality of  $C$  and  $A$  matrices. Thanks to the first preparatory sweep, the global error on the matrix product reduces to the local error on  $C^t$ .

The results in this work were obtained fixing the number of retained singular values  $M'$  for all iterations. Alternatively, given a target threshold  $\varepsilon$ , one can select  $M'$  adaptively such that, e.g.  $\frac{\lambda_{M'}}{\sqrt{\sum_k \lambda_k^2}} < \varepsilon$ , as in [9]. As a side remark, we point out that there exist techniques to compute directly the SVD truncated to the  $M'$  largest singular values [28, 29]. Such strategies can be advantageous for large matrix size and small  $M'$ .

The BP equations are iterated until convergence to a fixed point. It is worth noting that in the case of free dynamics one can build the messages incrementally from time 0 to time  $T$  as in DC (see e.g. [9]), with no need to iterate until convergence. Because each sweep of SVD over  $t$  matrices takes linear time in  $t$ , the total computational cost when using such scheme scales quadratically with  $T$ . Instead, initializing messages for all  $T$  epochs and then doing  $N_{\text{iter}}$  iterations as in our method takes  $\mathcal{O}(N_{\text{iter}} T)$ . The two are essentially equivalent since we observed that typically the number of iterations needed to converge is of the order of  $T$ . The procedure naturally lends itself to parallelization: outgoing messages can be computed independently for each node.

It is worth noting that, up to the errors introduced by the truncations, which we showed to be controlled, MPBP is exact on acyclic graphs.

*a. Observables* Single-variable and pair marginal distributions as well as time autocorrelations can be computed efficiently on a fixed point of BP by means of techniques analogue to those used in quantum MPS's (see appendix for details). The BP formalism also gives access to the Bethe Free Energy, an approximation to (minus the logarithm of) the normalization of (2), which can be interpreted as the likelihood of the parameters of the dynamics (e.g. infection rates, temperature,...). In cases where such parameters are unknown, they can be learned via a maximum-likelihood procedure.

*b. Thermodynamic limit* Just like standard BP, MPBP lends itself to be extended to infinite graphs. In the case of random regular graphs with homogeneous properties (e.g.  $\lambda_{ij} \equiv \lambda, \rho_i \equiv \rho$  for epidemic models,  $J_{ij} \equiv J, h_i \equiv h$  for Glauber dynamics), a single message is sufficient to represent the distribution in the thermodynamic limit. For graph ensembles with variable degree and/or parameters distributed according to some disorder, we adopt a population dynamics approach.

### C. A scheme to reduce the computational cost

As mentioned before, in the scheme proposed in [9], matrices before truncation have size  $M^{z-1}$  where  $M$  is the size of matrices in the incoming messages and  $z$  is the degree. The bottleneck are the sweeps of SVDs which yield a computational cost  $\mathcal{O}(M^{3z-3})$  for a single BP message. Although in a later work [10, , section 6] it was shown that such cost can be reduced to  $\mathcal{O}(M^{2z-1})$ , the exponential dependence on the degree still represents an issue even for graphs of moderately large connectivity. Here we show an improved scheme that, for a wide class of problems including epidemic modeling and some cases of Glauber dynamics, performs the computation in  $\mathcal{O}(M^6)$ . The dependence on  $z$  is only polynomial and depends on the details of the model.

It is enough to notice that in many cases transition probabilities  $w(x_i^{t+1}|\mathbf{x}_{\partial i}^t, x_i^t)$  depend on  $\mathbf{x}_{\partial i}^t$  only through some intermediate variable which incorporates the aggregate interaction with all the neighbors. In epidemic models like SI, SIR, SIRS, the transition probability only depends on the event that at least one of the neighbors has infected node  $i$ . In the case of Glauber dynamics the transition probability only depends on the local field, which is a weighted sum of neighboring spins.

More formally, consider intermediate scalar variables  $y_A^t$  with  $A \subseteq \partial i$  encoding information about  $\mathbf{x}_A^t$ . By definition of conditional probability

$$p(x_i^{t+1}|\mathbf{x}_{\partial i}^t, x_i^t) = \sum_{y_{\partial i}} p(x_i^{t+1}|y_{\partial i}^t, x_i^t) p(y_{\partial i}^t|\mathbf{x}_{\partial i}^t, x_i^t) \quad (19)$$

If it holds that

$$\begin{aligned} p(y_{A \cup B}^t | x_{A \cup B}^t, x_i^t) &= \sum_{y_A, y_B} p(y_{A \cup B}^t | y_A^t, y_B^t, x_i^t) \\ &\quad \times p(y_A^t, y_B^t | x_{\partial i}^t, x_i^t) \quad (20) \end{aligned}$$

$$= \sum_{y_A, y_B} p(y_{A \cup B}^t | y_A^t, y_B^t, x_i^t) \quad (21)$$

for  $A \cup B \subseteq \partial i$  (i.e. that the  $y$  of disjoint index sets are independent given the  $x$ 's), then it suffices to provide:

1.  $p(y_j^t | x_j^t, x_i^t)$
2.  $p(y_{A \cup B}^t | y_A^t, y_B^t, x_i^t)$

to be able to compute the set of outgoing messages from a node in a recursive manner. This is more efficient than the naive implementation provided that the number of values that each  $y$  can assume does not grow exponentially with the number of  $x$ 's it incorporates. More details of the computation can be found in the appendix.

## III. RESULTS

In this section we illustrate the effectiveness of MPBP applied to epidemic problems and Glauber dynamics. We first focus on free dynamics, showing results that are at least comparable with the existing methods, often more accurate. Then we move to reweighted processes, where our method really represents an innovation.

### A. Risk assessment in Epidemics

As examples of free dynamics, we estimate the marginal probability of an individual being in the infectious state under the SIS model, in several settings. On a random tree and on a diluted random graph, both of size  $N = 1000$ , MPBP shows almost no discrepancy with Monte Carlo averages (fig. 1a, 1b). In the former case a single node was picked as the sole infectious individual at time zero, in the latter a uniform probability  $\gamma_i \equiv \gamma$  was put on each node. As a comparison we report the curves obtained using a discrete-time version of the so-called Individual-Based Mean Field (IBMF) [1] and Dynamic message Passing (DMP) [24], which were originally devised for continuous time evolution (more details in the appendix). We evaluate the accuracy of each method by considering the average absolute error with respect to a Monte Carlo simulation  $\frac{1}{N} \sum_{i=1}^N |p(x_i^t = I) - p^{MC}(x_i^t = I)|$  (insets of fig. 1). The same analysis is repeated on Zachary's karate club network [30] (fig. 1c), the same benchmark used in [7, 24]. It must be pointed out that although MPBP shows by far the best performance in these comparison, the other considered methods are significantly simpler. None of the analytic methods is devised to analyze reweighted dynamics.

Finally, we compare MPBP against three continuous-time methods, DMP, IBMF and the Cavity Master Equation (CME), on the karate club graph. The comparison is made by multiplying the transmission and recovery rates for the continuous setting  $\lambda, \rho$  by the time-step  $\Delta t$  to turn them into probabilities to be handled by MPBP. MPBP gives the best overall prediction across the considered window.

Moving to reweighted processes, fig. 2 shows the efficacy of MPBP when performing inference of trajectories given some observations. On a small ( $N = 23$ ) random graph, a 10-step trajectory  $\bar{y}$  was sampled from a SIS prior distribution with  $\lambda = 0.15, \rho = 0.12, \gamma = 0.13$ . We then added observations  $\prod_{i \in I} \phi_i^T(x_i^T) = \prod_{i \in I} \delta(y_i^T x_i^T)$  over a random half  $I \subset V$  of the nodes and performed inference using (3). The MPBP estimate for the posterior marginals, obtained with matrices of size 3, agrees almost perfectly with Monte Carlo simulations. This is good indication that MPBP applied to sparse problems will keep giving accurate results even when on larger and/or more constrained instances where Monte Carlo methods fail,

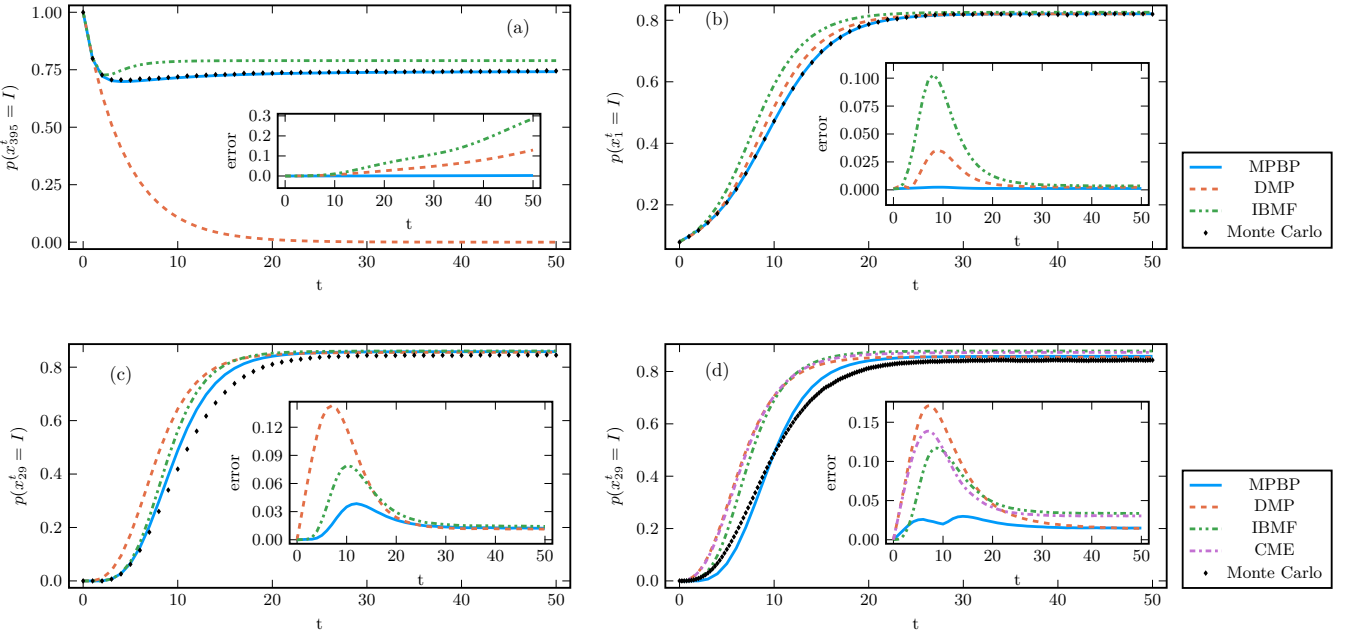


Figure 1. Marginal probabilities of free dynamics under the SIS model, comparison with models mentioned in the text. The main panels correspond to marginals for a single node of the graph, insets show the average absolute error over all nodes with respect to Monte Carlo simulations. Panels (a-c) compare against discretized versions of IBMF and DMP and the Monte Carlo strategy reported in the text, panel (d) against regular continuous-time versions and a Gillespie-like Monte Carlo simulation. (a) Marginal of node 395, the most connected one of a random tree with  $N = 1000$  nodes,  $\lambda = 0.3$ ,  $\rho = 0.2$ . Node 395 is the only infectious at time zero. Matrix size for MPBP: 12. (b) Marginal of node 1 of a ER graph with  $N = 1000$  nodes, average connectivity  $c = 5$ ,  $\lambda = 0.1$ ,  $\rho = 0.05$ ,  $\gamma = 0.08$ . Matrix size for MPBP: 10. (c) Marginal of node 29 (zero-based numbering to match previous works) of Zachary's karate club network,  $N = 34$  nodes,  $\lambda = 0.1$ ,  $\rho = 0.05$ , node 0 is the only infectious at time zero. Matrix size for MPBP: 10. (d) Same as (c) but the comparison is with continuous-time methods, with the addition of CME.

leaving little to compare against.

Realistic scenarios are often better described by the Susceptible-Infectious-Recovered-Susceptible (SIRS) model where transmission of infections is analogous to the SIS case, but an infectious node  $i$  can recover with probability  $\rho_i$  and a recovered become susceptible again with probability  $\sigma_i$ . From a practical point of view, extending the SIR to SIRS in the MPBP framework takes little effort: it suffices to enrich the factors with the new transition  $R \rightarrow S$ . Fig. (3) shows the performance of MPBP at estimating the posterior trajectories for a single realization of an epidemic drawn from a prior whose parameters  $\lambda, \rho, \sigma, \gamma$  are homogeneous and known. A random 75% of the system was observed at an intermediate time (colored dots). We see good agreement between the true infection times (black lines) and the marginal probabilities of being Infectious (in yellow). Nodes are sorted in increasing order of true first infection time.

## B. Kinetic Ising

As examples of free dynamics we consider the evolution of magnetization  $\langle \sigma_i^t \rangle$  and time autocovariance  $\langle \sigma_i^t \sigma_i^s \rangle - \langle \sigma_i^t \rangle \langle \sigma_i^s \rangle$  for pairs of epochs  $(t, s)$ , on ferromag-

netic, Random Field and spin-glass Ising Models (fig. 4). First we consider a model with uniform couplings  $J_{ij} \equiv J$  on an infinite Random Regular Graph like the one studied in [9] but with degree 8 instead of 3. We then apply our method to an infinite Erdos-Renyi graph, again with uniform couplings and in the ferromagnetic phase, using a population dynamics approach. Next, we study a Random Field Ising Model (RFIM) with uniform couplings and random external fields  $h_i = \pm h$  on a large graph. In all three cases the system is initialized in a magnetized state and the fraction of up spins grows or decreases monotonically until it reaches its equilibrium value. For these second and third models we picked the same settings as in [25]. Finally, we consider an anti-ferromagnetic model with  $J = -1$  at zero temperature ( $\beta = \infty$ ), focusing on the nearest-neighbor correlation  $\langle \sigma_i^t \sigma_j^t \rangle$ ,  $(i, j) \in E$  rather than the magnetization, which is null at steady state. Above the critical inverse temperature  $\beta_c = \log(1 + \sqrt{2})$  [31], the system is in a glassy phase and, as expected, Glauber dynamics fails at finding the correct ground state. Indeed, the 1RSB prediction [32] (dashed line) gives a lower estimate for the average correlation, which also corresponds to the ground state energy. For this model we used the modified version of the dynamics reported in (6) with  $p_0 = 0.25$ .

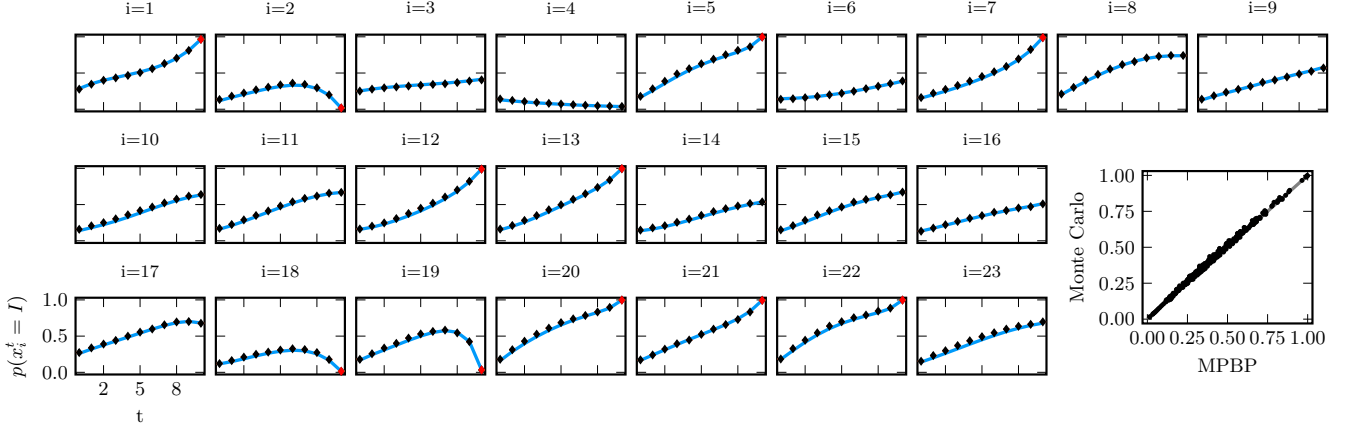


Figure 2. MPBP (solid line) with matrix size 3 correctly computes marginals of an SIS model defined on an Erdos-Renyi graph with 23 nodes and average connectivity 4,  $\lambda = 0.15, \rho = 0.12, \gamma = 0.13$ . A random half of the variables were observed at final time  $T = 10$  (red dots). Black dots are the average over  $10^6$  Monte Carlo simulations. (Bottom-right) Comparison of all points from the previous plots, the Pearson correlation coefficient is 0.9986.

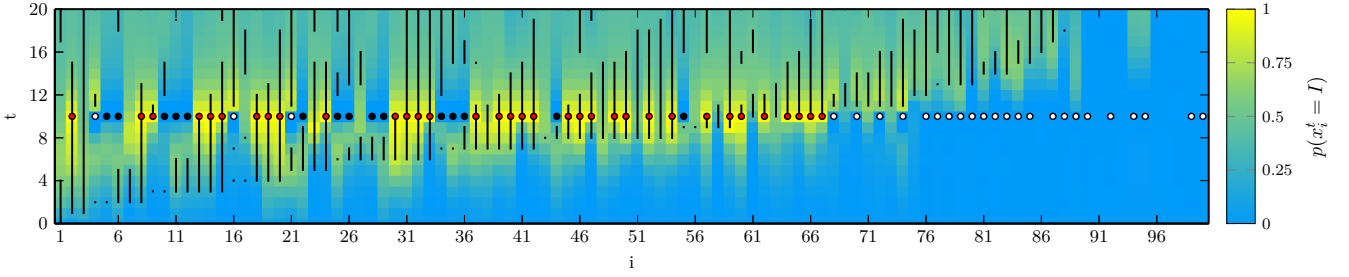


Figure 3. Inference on a single epidemic outbreak sampled from a SIRS model on an Erdos-Renyi graph with average connectivity  $c = 2.5, N = 100$ . The process to be inferred was drawn from a SIRS prior with  $\lambda = 0.4, \rho = \sigma = 0.15, \gamma = 0.01$ , the same parameters were used for the inference. 75% of the nodes were observed at time 10 (white=S, red=I, black=R). Matrix size for MPBP  $M = 3$ . Black lines correspond to true infection periods.

We study the large deviation behavior of a free dynamic  $W(\bar{\sigma}) = \prod_{i=1}^N w(\sigma_i^0) \prod_{t=0}^{T-1} w(\sigma_i^{t+1} | \sigma_{\partial i}^t)$  by tilting it with an external field at final time  $\prod_i \phi_i^T(\sigma_i^T) = \prod_i e^{h\sigma_i^T}$ . In the thermodynamic limit  $N \rightarrow \infty$  this allows to select a particular value for the magnetization at final time  $m = \frac{1}{N} \sum_i \sigma_i^T$ . The Bethe Free Energy computed via MPBP is an approximation for

$$f(h) = -\frac{1}{N} \log \sum_{\{\sigma_i^t\}_{i,t}} W(\bar{\sigma}) e^{h \sum_i \sigma_i^T} \quad (22)$$

$$= -\frac{1}{N} \log \sum_m e^{-N[g(m) - hm]} \quad (23)$$

$$\xrightarrow{N \rightarrow \infty} \min_m \{g(m) - hm\} \quad (24)$$

$$= g(m(h)) - hm(h) \quad (25)$$

where  $g(m) = -\frac{1}{N} \log \sum_{\{\sigma_i^t\}_{i,t}} W(\bar{\sigma}) \delta(Nm, \sum_i \sigma_i^T)$ , and  $m(h) = \arg \min_m \{g(m) - hm\}$ . In regions where  $g(m)$  is convex, the Legendre transform (24) can be in-

verted to obtain a large deviation law for the probability of observing the system at final time with magnetization  $m$

$$p(m) \sim e^{-N[g(h(m)) + mh(m)]} \quad (26)$$

where  $h(m)$  is the inverse of  $m(h)$ . Fig. 5 shows the estimate of  $g(m)$  for a ferromagnetic Ising model on an infinite random graph initialized at magnetization  $m^0 = 0.1$  and evolving according to Glauber dynamics for  $T = 10$  epochs.  $p(m)$  has a minimum at  $m \approx 0.145$  which corresponds to the free dynamics  $h = 0$ .

Such an analysis could not have been carried out by means of Monte Carlo methods since the probability of sampling a trajectory ending at  $m$  is infinitesimal, as is clear from the large deviation law in fig. 5.

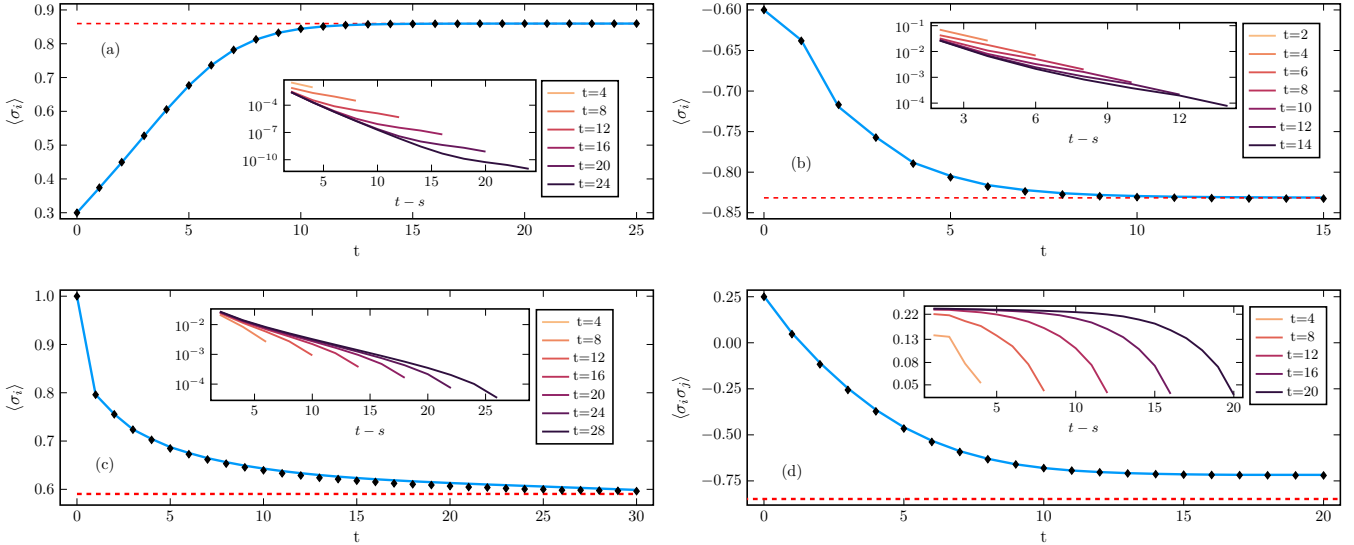


Figure 4. Magnetization  $\langle \sigma_i^t \rangle$  (a-c) or nearest-neighbor correlation  $\langle \sigma_i^t \sigma_j^t \rangle$  (d) as a function of time for different Ising models. Solid lines are MPBP, dots are Monte Carlo simulations on graphs of size  $N_{MC}$ , dashed horizontal lines are the equilibrium values (a-c) or 1RSB prediction (d) for the corresponding static versions of the models. Insets show autocovariances  $\langle \sigma_i^t \sigma_i^s \rangle - \langle \sigma_i^t \rangle \langle \sigma_i^s \rangle$ , only even epochs are shown for panels (a-c) because of odd-even effects in the dynamics of ferromagnetic models (as in [9, 25]). (a) Infinite 8-Random Regular Graph,  $\beta J = 0.2$ ,  $N_{MC} = 5000$ , matrix size 25. (b) Infinite Erdos-Renyi graph with mean connectivity  $c = 4$ ,  $\beta J = 0.5$ ,  $N_{MC} = 5000$ , matrix size 18. (c) Random Field Ising Model on Erdos-Renyi graph with mean connectivity  $c = 3$ ,  $\beta J = 2/c$ ,  $N = N_{MC} = 1000$  and  $\beta h_i = \pm 0.6$  sampled uniformly, matrix size 10. (d) Antiferromagnetic Ising Model on infinite 3-Random Regular Graph with  $J = -1$ ,  $\beta = \infty$ ,  $N_{MC} = 5000$ , matrix size 23.

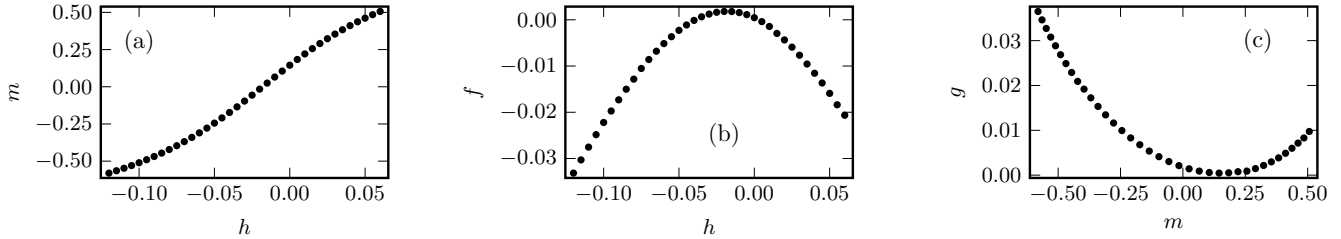


Figure 5. Large deviation study of Glauber dynamics on an infinite 3-Random Regular Graph. Free dynamics with  $\beta J = 0.6$ ,  $T = 10$ , magnetization at time zero  $m^0 = 0.1$ , zero external field, reweighted with an external field at final time  $\prod_i \phi_i^T(\sigma_i^T) = \prod_i e^{h \sigma_i^T}$ . (a) Magnetization vs reweighting field, (b) Bethe Free Energy vs reweighting field, (c) Magnetization-constrained free energy  $g(m)$  vs magnetization. Matrix size for MPBP: 25.

#### IV. DISCUSSION

It is often the case that stochastic processes which can be described accurately, be it by analytical or Monte-Carlo methods, become computationally difficult as soon as the dynamics is biased by some reweighting factor. This constitutes a massive limitation since reweighting is essential whenever one is interested in describing atypical trajectories, an emblematic example being inference in epidemic models. As of today there exist, to the best of our knowledge, no analytic method able to describe reweighted complex dynamics on networks except for the simple case of non-recurrent models. In this article we adopted the matrix-product parametrization, inspired by

techniques used originally in quantum physics and recently applied to classical stochastic dynamics in [9], to devise the Matrix Product Belief Propagation method. We used it to describe reweighted Markov dynamics on graphs, and applied it to epidemic spreading and a dynamical Ising models. With respect to the important work in [9, 10], which we recall that applies only to free dynamics, our contribution is twofold.

First, we develop for MPBP a general scheme to render the computation time linear in the node degree rather than exponential on a wide class of models, allowing us to compare it extremely favorably with existing methods on standard benchmark examples (which typically include vertices with large degrees). The bottleneck of the whole

computation in the final scheme is due to the SVD factorization, which are cubic in the size  $M$  of the matrices: larger matrices give a better approximation, but require a greater computational effort. The overall cost per iteration, assuming the matrix size constant, is  $O(T|E|)$ , i.e. linear in the number of edges of the graph. A small number of iterations is normally sufficient for approximate convergence a fixed point. It is fair to point out, however, that although linear, depending on the target accuracy of the approximation defined by the parameter  $M$ , the method may be substantially more computationally intensive than the others used for comparison.

Second and more importantly, the MPBP approach allows to include reweighting factors. In particular, the approach proposed in [9, 10] is iterated forward in (dynamical) time, and thus allows no backward flow of information which is necessary with reweighting factors. Reweighting factors are necessary to analyze conditioned dynamics and rare events.

MPBP, like many other statistical physics-inspired approaches to stochastic dynamics, is based on the cavity approximation. The Belief Propagation formalism gives access to the thermodynamic limit for certain ensembles of random graphs, provides an approximation to the partition function through the Bethe Free Energy, and allows to compute time autocorrelations. The limits of validity of MPBP are inherited from those of the cavity approximation: using the jargon of disordered systems, the approximation is accurate as long as the problem is in a *Replica Symmetric* (RS) phase. In the case of epidemic inference presented in fig. 3 this is surely the case, since the trajectory to be inferred was sampled from the same

prior used for the inference. This amounts to working on the Nishimori line, where it is known that no replica symmetry-breaking takes place [33]. A study of the performance in regimes where replica symmetry is broken is left for future investigation.

On graphs with short loops, the performance of BP degrades substantially. In the static case, this issue can sometimes be overcome by resorting to higher order approximations [34]. We argue that the same ideas can be translated to dynamics, for example by describing explicitly the joint trajectory of quadruples of neighboring variables on a square lattice.

Software implementing the method is available at [19] and can be used to directly reproduce the results in the article. The framework is flexible and accommodates for the inclusion of new models of dynamics.

As a final remark, we recall that the method applies more in general to any distribution of the type (1), where  $t$  need not be interpreted as a time index but could, for instance, span a further spatial direction. Investigation along this line is left for future work.

## ACKNOWLEDGMENTS

This study was carried out within the FAIR - Future Artificial Intelligence Research and received funding from the European Union Next-GenerationEU (Piano Nazionale di Ripresa e Resilienza (PNRR) – Missione 4 Componente 2, Investimento 1.3 – D.D. 1555 11/10/2022, PE00000013). This manuscript reflects only the authors' views and opinions, neither the European Union nor the European Commission can be considered responsible for them.

---

[1] P. Van Mieghem, J. Omic, and R. Kooij, IEEE/ACM Transactions On Networking **17**, 1 (2008).

[2] B. Karrer and M. E. Newman, Physical Review E **82**, 016101 (2010).

[3] G. Del Ferraro and E. Aurell, Phys. Rev. E **92**, 010102 (2015).

[4] A. Pelizzola, The European Physical Journal B **86**, 1 (2013).

[5] A. Pelizzola and M. Pretti, Journal of Statistical Mechanics: Theory and Experiment **2017**, 073406 (2017).

[6] E. Aurell, G. Del Ferraro, E. Domínguez, and R. Mulet, Phys. Rev. E **95**, 052119 (2017).

[7] E. Ortega, D. Machado, and A. Lage-Castellanos, Phys. Rev. E **105**, 024308 (2022).

[8] I. Neri and D. Bollé, Journal of Statistical Mechanics: Theory and Experiment **2009**, P08009 (2009).

[9] T. Barthel, C. De Bacco, and S. Franz, Physical Review E **97**, 010104 (2018).

[10] T. Barthel, Journal of Statistical Mechanics: Theory and Experiment **2020**, 013217 (2020).

[11] D. Perez-Garcia, F. Verstraete, M. M. Wolf, and J. I. Cirac, Quantum Info. Comput. **7**, 401 (2007).

[12] F. Verstraete and J. I. Cirac, Physical review b **73**, 094423 (2006).

[13] M. Fannes, B. Nachtergael, and R. F. Werner, Communications in mathematical physics **144**, 443 (1992).

[14] B. Derrida, M. R. Evans, V. Hakim, and V. Pasquier, Journal of Physics A: Mathematical and General **26**, 1493 (1993).

[15] M. C. Bañuls and J. P. Garrahan, Physical review letters **123**, 200601 (2019).

[16] Z.-Y. Han, J. Wang, H. Fan, L. Wang, and P. Zhang, Physical Review X **8**, 031012 (2018).

[17] E. Stoudenmire and D. J. Schwab, Advances in neural information processing systems **29** (2016).

[18] F. Altarelli, A. Braunstein, L. Dall'Asta, and R. Zecchina, Physical Review E **87**, 062115 (2013).

[19] S. Crott and A. Braunstein, “MatrixProductBP,” <https://github.com/stecrotti/MatrixProductBP> (2023), will be made available after publication.

[20] A. Renart, J. De La Rocha, P. Bartho, L. Hollender, N. Parga, A. Reyes, and K. D. Harris, science **327**, 587 (2010).

[21] Y. Roudi and J. Hertz, Physical review letters **106**, 048702 (2011).

[22] H. Ohta and S.-i. Sasa, Europhysics Letters **90**, 27008 (2010).

[23] P. Van Mieghem, Computing **93**, 147 (2011).

- [24] M. Shrestha, S. V. Scarpino, and C. Moore, Physical Review E **92**, 022821 (2015).
- [25] E. D. Vázquez, G. Del Ferraro, and F. Ricci-Tersenghi, Journal of Statistical Mechanics: Theory and Experiment **2017**, 033303 (2017).
- [26] G. Del Ferraro and E. Aurell, Journal of the Physical Society of Japan **83**, 084001 (2014).
- [27] N. Antulov-Fantulin, A. Lančić, T. Šmuc, H. Štefančić, and M. Šikić, Physical review letters **114**, 248701 (2015).
- [28] R. M. Larsen, DAIMI Report Series (1998).
- [29] J. Baglama and L. Reichel, SIAM Journal on Scientific Computing **27**, 19 (2005).
- [30] J. Kunegis, “Zachary karate club,” <http://konekt.cc/networks/ucidata-zachary/>, accessed: 14.01.2023.
- [31] A. Coja-Oghlan, P. Loick, B. F. Mezei, and G. B. Sorkin, SIAM Journal on Discrete Mathematics **36**, 1306 (2022).
- [32] L. Zdeborová and S. Boettcher, Journal of Statistical Mechanics: Theory and Experiment **2010**, P02020 (2010).
- [33] Y. Iba, Journal of Physics A: Mathematical and General **32**, 3875 (1999).
- [34] J. S. Yedidia, W. Freeman, and Y. Weiss, Advances in neural information processing systems **13** (2000).
- [35] F. Altarelli, A. Braunstein, L. Dall'Asta, A. Lage-Castellanos, and R. Zecchina, Physical review letters **112**, 118701 (2014).

## Appendix A: Details of the BP equations

Equation (12), with matrix indices and the special cases  $t = 0, T$  made explicit, reads

$$[B_{i \rightarrow j}^0(x_i^1, x_i^0, x_j^0)]_{\{a_k^1\}_{k \in \partial i \setminus j}} = \sum_{\{x_k^0\}_{k \in \partial i \setminus j}} f_i^1(x_i^1 | \mathbf{x}_{\partial i}^0, x_i^0) \prod_{k \in \partial i \setminus j} [A_{k \rightarrow i}^0(x_k^0, x_i^0)]_{a_k^1} \quad (\text{A1})$$

$$[B_{i \rightarrow j}^t(x_i^{t+1}, x_i^t, x_j^t)]_{\{a_k^t, a_{t+1}^k\}_{k \in \partial i \setminus j}} = \sum_{\{x_k^t\}_{k \in \partial i \setminus j}} f_i^{t+1}(x_i^{t+1}, \mathbf{x}_{\partial i}^t, x_i^t) \prod_{k \in \partial i \setminus j} [A_{i \rightarrow j}^t(x_k^t, x_i^t)]_{a_k^t, a_{k+1}^{t+1}} \quad \forall t \in \{1, \dots, T-1\} \quad (\text{A2})$$

$$[B_{i \rightarrow j}^T(x_i^T, x_j^T)]_{\{a_k^T\}_{k \in \partial i \setminus j}} = \sum_{\{x_k^T\}_{k \in \partial i \setminus j}} \prod_{k \in \partial i \setminus j} [A_{k \rightarrow i}^T(x_k^T, x_i^T)]_{a_k^T} \quad (\text{A3})$$

## Appendix B: How to perform SVD on a tensor

SVD is only defined for matrices, i.e. arrays with two indices. Whenever one wishes to apply it to tensors (intended not in the differential-geometric sense, but as arrays of dimension higher than two), indices must be split into two subsets and treated as “macro-indices” of a new matrix. In computer science lingo, one *reshapes* the high-dimensional array into a two-dimensional one. For instance, the SVD in (13) in full detail reads

$$[B_{i \rightarrow j}^t(x_i^{t+1}, x_i^t, x_j^t)]_{\underline{a}^t, \underline{a}^{t+1}} \stackrel{\text{SVD}}{=} \sum_{k=1}^K [C_{i \rightarrow j}^t(x_i^t, x_j^t)]_{\underline{a}^t, k} \Lambda_{kk} [V^\dagger(x_i^{t+1})]_{k, \underline{a}^{t+1}} \quad (\text{B1})$$

where  $(x_i^t, x_j^t, \underline{a}^t)$  are treated as a macro-index for the rows of  $B$  and  $(x_i^{t+1}, \underline{a}^{t+1})$  the macro-index for the columns. The range of values for  $k$  is determined by the minimum between the number of rows and columns of  $B$ :

$$K = \min \left\{ q^2 M^{|\partial i|-1}, q M^{|\partial i|-1} \right\} \quad (\text{B2})$$

where  $M$  is the matrix size of the incoming messages, for simplicity supposed equal for all neighbors and times. Analogously, 16 in detail reads

$$[C_{i \rightarrow j}^t(x_i^t, x_j^t)]_{\underline{a}^t, \underline{a}^{t+1}} \stackrel{\text{SVD,trunc}}{=} \sum_{k=1}^M U_{\underline{a}^t, k} \Lambda_{kk} [A_{i \rightarrow j}^t(x_i^t, x_j^t)]_{k, \underline{a}^{t+1}}. \quad (\text{B3})$$

Finally, the orthonormality property (15) with explicit indices reads:

$$\sum_{x_i^t, x_j^t, \underline{a}^t} [C_{i \rightarrow j}^t(x_i^t, x_j^t)]_{\underline{a}^t, k} [C_{i \rightarrow j}^t(x_i^t, x_j^t)]_{\underline{a}^t, k'} = \delta(k, k') \quad (\text{B4})$$

## Appendix C: Evaluation of observables

Given a joint distribution in matrix product form

$$p(x^0, x^1, \dots, x^T) = \frac{1}{Z} \sum_{a^1, a^2, \dots, a^T} [A^0(x^0)]_{a^1} [A^1(x^1)]_{a^1, a^2} \cdots [A^{T-1}(x^{T-1})]_{a^{T-1}, a^T} [A^T(x^T)]_{a^T} \quad (\text{C1})$$

one can efficiently compute: normalization, marginals, autocorrelations.

a. *Normalization and marginals* Marginalizing at time  $t$  gives

$$p^t(x^t) = \sum_{\{x^s\}_{s \neq t}} p(x^0, x^1, \dots, x^T) \quad (\text{C2})$$

$$= \frac{1}{Z} \sum_{a^t, a^{t+1}} [L^{t-1}]_{a^t} [A^t(x^t)]_{a^t, a^{t+1}} [R^{t+1}]_{a^{t+1}} \quad (\text{C3})$$

where we defined partial normalizations from the left and from the right

$$\begin{cases} [L^t]_{a^{t+1}} := \sum_{a^1, \dots, a^t} \prod_{s=0}^t \sum_{x^s} [A^s(x^s)]_{a^s, a^{s+1}} \\ [R^t]_{a^t} := \sum_{a^{t+1}, \dots, a^T} \prod_{s=t}^T \sum_{x^s} [A^s(x^s)]_{a^s, a^{s+1}} \end{cases} \quad (\text{C4})$$

with initial conditions

$$\begin{cases} [L^0]_{a^1} := \sum_{x^0} [A^0(x^0)]_{a^1} \\ [R^T]_{a^T} := \sum_{x^T} [A^T(x^T)]_{a^T} \end{cases} \quad (\text{C5})$$

The normalization is given by

$$Z = \sum_{a^t} [L^t]_{a^{t+1}} [R^{t+1}]_{a^{t+1}} \quad \forall t \in 0, 1, \dots, T-1. \quad (\text{C6})$$

b. *Autocorrelations* Further define “middle” partial normalizations from  $t$  to  $s$  ( $t < s$  without loss of generality)

$$[M^{t,s}]_{a^{t+1}, a^u} = \sum_{a^{t+2}, \dots, a^{u-1}} \prod_{u=t+1}^{s-1} \sum_{x_i^u, x_f^u} [A^u(x^u)]_{a^u, a^{u+1}} \quad (\text{C7})$$

$$= \sum_{a^{s-1}} [M^{t,s-1}]_{a^{t+1}, a^{s-1}} \left( \sum_{x^{u-1}} [A^{s-1}(x^{s-1})]_{a^{s-1}, a^s} \right) \quad (\text{C8})$$

with initial condition

$$[M^{t,t+1}]_{a,b} = \delta(a, b) \quad \forall t \in \{0, 1, \dots, T-1\}. \quad (\text{C9})$$

Now

$$p^{t,s}(x^t, x^s) = \sum_{\{x^u\}_{u \neq t,s}} p(x^0, x^1, \dots, x^T) \quad (\text{C10})$$

$$= \frac{1}{Z} \sum_{\substack{a^t, a^{t+1} \\ a^s, a^{s+1}}} [L^{t-1}]_{a^t} [A^t(x^t)]_{a^t, a^{t+1}} [M^{t,s}]_{a^{t+1}, a^s} [A^s(x^s)]_{a^s, a^{s+1}} [R^{s+1}]_{a^{s+1}}. \quad (\text{C11})$$

## Appendix D: Bethe Free Energy

The Bethe Free Energy for a graphical model with pair-wise interactions is given by

$$F_{\text{Bethe}} = - \sum_i \log z_i + \frac{1}{2} \sum_i \sum_{j \in \partial i} \log z_{ij} \quad (\text{D1})$$

where

$$z_i = \sum_{\bar{x}_i, \bar{x}_{\partial i}} \prod_{t=0}^{T-1} f_i^{t+1}(x_i^{t+1} | \mathbf{x}_{\partial i}, x_i^t) \prod_{k \in \partial i} m_{k \rightarrow i}(\bar{x}_k, \bar{x}_i) \quad (\text{D2})$$

$$z_{ij} = \sum_{\bar{x}_i, \bar{x}_j} m_{i \rightarrow j}(\bar{x}_i, \bar{x}_j) m_{j \rightarrow i}(\bar{x}_j, \bar{x}_i). \quad (\text{D3})$$

It is useful to define

$$z_{i \rightarrow j} = \sum_{\bar{x}_i, \bar{x}_j} \sum_{\bar{x}_{\partial i \setminus j}} \prod_{t=0}^{T-1} f_i^{t+1}(x_i^{t+1} | \mathbf{x}_{\partial i}^t, x_i^t) \prod_{k \in \partial i \setminus j} m_{k \rightarrow i}(\bar{x}_k, \bar{x}_i) = \frac{z_i}{z_{ij}}. \quad (\text{D4})$$

Finally,

$$F_{\text{Bethe}} = \sum_i \left[ \left( \frac{d_i}{2} - 1 \right) \log z_i - \frac{1}{2} \sum_{j \in \partial i} \log z_{i \rightarrow j} \right] \quad (\text{D5})$$

The Bethe free energy can be obtained using only  $\{z_i\}$ ,  $\{z_{i \rightarrow j}\}$ , which are already computed when normalizing messages during the BP iterations.

### Appendix E: Efficient BP computations

We give here details of the efficient procedure for the computation of BP messages mentioned in the main text. Re-writing the BP equation (omitting for clarity the  $\phi$  terms) in terms of the auxiliary variables  $\{y_A^t\}_{A \subseteq \partial i}$  gives

$$m_{i \rightarrow j}(\bar{x}_i, \bar{x}_j) \propto \sum_{\bar{x}_{\partial i \setminus j}} \prod_t w(x_i^{t+1} | \mathbf{x}_{\partial i \setminus j}^t, x_i^t, x_j^t) \prod_{k \in \partial i \setminus j} m_{k \rightarrow i}(\bar{x}_k, \bar{x}_i) \quad (\text{E1})$$

$$\propto \sum_{\bar{x}_{\partial i \setminus j}} \sum_{\bar{y}_{\partial i \setminus j}} \prod_t p(x_i^{t+1} | y_{\partial i \setminus j}^t, x_i^t, x_j^t) p(y_{\partial i \setminus j}^t | \mathbf{x}_{\partial i \setminus j}^t, x_i^t) \prod_{k \in \partial i \setminus j} m_{k \rightarrow i}(\bar{x}_k, \bar{x}_i) \quad (\text{E2})$$

$$\propto \sum_{\bar{y}_{\partial i \setminus j}} \prod_t p(x_i^{t+1} | y_{\partial i \setminus j}^t, x_i^t, x_j^t) \tilde{m}_{\partial i \setminus j \rightarrow i}(\bar{y}_{\partial i \setminus j}, \bar{x}_i) \quad (\text{E3})$$

where we defined  $\tilde{m}_{\partial i \setminus j \rightarrow i}(\bar{y}_{\partial i \setminus j}, \bar{x}_i) = \sum_{\bar{x}_{\partial i \setminus j}} \prod_t p(y_{\partial i \setminus j}^t | \mathbf{x}_{\partial i \setminus j}^t, x_i^t) \prod_{k \in \partial i \setminus j} m_{k \rightarrow i}(\bar{x}_k, \bar{x}_i)$ .

Now  $\tilde{m}_{\partial i \setminus j \rightarrow i}$  can be computed as the aggregation of all messages  $\tilde{m}_{k \rightarrow i}$  with  $k < j$  and messages  $\tilde{m}_{k \rightarrow i}$  with  $k > j$ :

$$\tilde{m}_{\partial i \setminus j \rightarrow i}(\bar{y}_{\partial i \setminus j}, \bar{x}_i) = \sum_{\bar{y}_{< j}} \sum_{\bar{y}_{> j}} \prod_t p(y_{\partial i \setminus j}^t | y_{< j}^t, y_{> j}^t, x_i^t) \tilde{m}_{< j}(\bar{y}_{< j}, \bar{x}_i) \tilde{m}_{> j}(\bar{y}_{> j}, \bar{x}_i) \quad (\text{E4})$$

where we used the short-hand notation  $\leqslant j = \{k \in \partial i \setminus j, k \leqslant j\}$ . The last equation is naturally cast to matrix product form with

$$\left[ \tilde{A}_{\partial i \setminus j \rightarrow i}^t(y_{\partial i \setminus j}^t, x_i^t) \right]_{(a^t, b^t), (a^{t+1}, b^{t+1})} = \sum_{y_{< j}^t} \sum_{y_{> j}^t} p(y_{\partial i \setminus j}^t | y_{< j}^t, y_{> j}^t, x_i^t) \left[ \tilde{A}_{< j}(y_{< j}^t, x_i^t) \right]_{a^t, a^{t+1}} \left[ \tilde{A}_{> j}(y_{> j}^t, x_i^t) \right]_{b^t, b^{t+1}} \quad (\text{E5})$$

where subscripts for the matrices match those of the corresponding messages in (E4). Matrices on the LHS have size double than those at RHS, therefore we perform the same SVD-based truncations explained in the main text. This is where the computational bottleneck lies: suppose that the incoming matrices have size  $M \times M$ . Performing a SVD on  $\tilde{A}_{\partial i \setminus j \rightarrow i}^t$ , reshaped as a matrix with  $(a^t, b^t)$  as row index and  $(a^{t+1}, b^{t+1}, y_{\partial i \setminus j}^t, x_i^t)$  as column index, costs  $\mathcal{O}(nM^6)$  where  $n$  is the number of values taken by  $y_{\partial i \setminus j}^t$  and depends on the model. As long as  $n$  depends at most polynomially on the degree  $z = |\partial i|$ , the exponential dependence is avoided.

Messages  $\tilde{m}$  can be computed recursively after having noticed that they satisfy analogous properties to (21):

$$\tilde{m}_{A \cup B}(\bar{y}_{A \cup B}, \bar{x}_i) = \sum_{\bar{y}_A, \bar{y}_B} \prod_t p(y_{A \cup B}^t | y_A^t, y_B^t, x_i^t) \tilde{m}_A(\bar{y}_A, \bar{x}_i) \tilde{m}_B(\bar{y}_B, \bar{x}_i) \quad (\text{E6})$$

starting from  $\tilde{m}_{\{k\} \rightarrow i}(\bar{y}_{\{k\}}, \bar{x}_i) = \sum_{\bar{x}_k} \prod_t p(y_{\{k\}}^t | x_k^t, x_i^t) m_{k \rightarrow i}(\bar{x}_k, \bar{x}_i)$  and  $\tilde{m}_{\emptyset \rightarrow i}(\bar{y}_\emptyset, \bar{x}_i) \propto 1 \forall (\bar{y}_\emptyset, \bar{x}_i)$ . Finally, we use (E3) to compute  $m_{i \rightarrow j}(\bar{x}_i, \bar{x}_j)$  for all  $j$ : just as in (12) we get matrices with dependency on both  $x_i^{t+1}$  and  $x_i^t$

$$B_{i \rightarrow j}^t(x_i^{t+1}, x_i^t, x_j^t) = \sum_{y_{\partial i \setminus j}^t} p(x_i^{t+1} | y_{\partial i \setminus j}^t, x_i^t, x_j^t) \tilde{A}_{\partial i \setminus j \rightarrow i}(y_{\partial i \setminus j}^t, x_i^t) \quad (\text{E7})$$

which are treated in the same way as explained in the main text for the generic BP implementation. At this point one can use the already computed quantities to retrieve the belief at node  $i$

$$b_i(\bar{x}_i) \propto \sum_{\bar{y}_{\partial i}} \prod_t p(x_i^{t+1} | y_{\partial i}^t, x_i^t) \tilde{m}_{\partial i \rightarrow i}(\bar{y}_{\partial i}, \bar{x}_i) \quad (\text{E8})$$

with  $j$  being any neighbor of  $i$ .

The strategy just described is summarized in algorithm 1. The procedure is manifestly linear in the degree, for an overall cost of  $\mathcal{O}(znM^6)$  for the update of all messages outgoing from a node. In cases where there exists no convenient choice for the auxiliary variables  $y$ , the scheme could still be implemented with  $y_A^t = \otimes_{a \in A} \{x_A^t\}$  and  $n \sim q^z$ : unsurprisingly, one recovers the exponential cost with respect to the degree.

---

**Algorithm 1** Efficient computation of outgoing messages and belief for a generic node  $i$ .

---

- for  $j \in \partial i$ 
  - $\tilde{m}_{\{k\} \rightarrow i}(\bar{y}_{\{k\}}, \bar{x}_i) \leftarrow \sum_{\bar{y}_k} \prod_t p(y_{\{k\}}^t | x_k^t, x_i^t) m_{k \rightarrow i}(\bar{y}_k, \bar{x}_i)$
  - $\tilde{m}_{\emptyset \rightarrow i}(\bar{y}_\emptyset, \bar{x}_i) \leftarrow 1$
- for  $j \in \partial i$ 
  - $\tilde{m}_{<j}(\bar{y}_{<j}, \bar{x}_i) \leftarrow \sum_{\bar{y}_{<j-1}} \sum_{\bar{y}_{\{j-1\}}} \prod_t p(y_{<j}^t | y_{<j-1}^t, y_{\{j-1\}}^t, x_i^t) \tilde{m}_{<j-1}(\bar{y}_{<j-1}, \bar{x}_i) \tilde{m}_{\{j-1\}}(\bar{y}_{\{j-1\}}, \bar{x}_i)$
  - $\tilde{m}_{>j}(\bar{y}_{>j}, \bar{x}_i) \leftarrow \sum_{\bar{y}_{>j+1}} \sum_{\bar{y}_{\{j+1\}}} \prod_t p(y_{>j}^t | y_{>j+1}^t, y_{\{j+1\}}^t, x_i^t) \tilde{m}_{>j+1}(\bar{y}_{>j+1}, \bar{x}_i) \tilde{m}_{\{j+1\}}(\bar{y}_{\{j+1\}}, \bar{x}_i)$
- for  $j \in \partial i$ 
  - $\tilde{m}_{\partial i \setminus j \rightarrow i}(\bar{y}_{\partial i \setminus j}, \bar{x}_i) \leftarrow \sum_{\bar{y}_{<j}} \sum_{\bar{y}_{>j}} \prod_t p(y_{\partial i \setminus j}^t | y_{<j}^t, y_{>j}^t, x_i^t) \tilde{m}_{<j}(\bar{y}_{<j}, \bar{x}_i) \tilde{m}_{>j}(\bar{y}_{>j}, \bar{x}_i)$
  - $m_{i \rightarrow j}(\bar{x}_i, \bar{x}_j) \leftarrow \sum_{\bar{y}_{\partial i \setminus j}} \prod_t p(x_i^{t+1} | y_{\partial i \setminus j}^t, x_i^t, x_j^t) \tilde{m}_{\partial i \setminus j \rightarrow i}(\bar{y}_{\partial i \setminus j}, \bar{x}_i)$

---

a. *Glauber and SIS* For Glauber dynamics the most general setting where these simplifications apply is couplings with constant absolute value  $|J_{ij}| \equiv J$  and arbitrary external fields, often referred to as the  $\pm J$  Ising model. The case with  $J_{ij} \equiv J$ ,  $h = 0$  studied in [9] is automatically covered. The transition probability (5) takes the form

$$e^{\beta \sigma_i^{t+1} [J(\sum_{j \in \partial i} \text{sign}(J_{ij}) \sigma_j^t) + h_i]} \propto e^{\beta \sigma_i^{t+1} [J(y_{\partial i \setminus j}^t + \text{sign}(J_{ij}) \sigma_j^t) + h_i]} \quad (\text{E9})$$

with  $y_A^t = \sum_{k \in A} \text{sign}(J_{ik}) \sigma_k^t$ . It is easy to see that  $p(y_{\{k\}}^t | \sigma_k^t, \sigma_i^t) = \mathbb{1}(y_{\{k\}}^t = \text{sign}(J_{ik}) \sigma_k^t)$  and  $p(y_{A \cup B}^t | y_A^t, y_B^t, \sigma_i^t) = \delta(y_{A \cup B}^t = y_A^t + y_B^t)$ . In this case,  $y_A^t$  can take value  $-|A|, -|A| + 2, \dots, |A| - 2, |A|$ , for a total  $2|A| + 1$  values. The maximum is achieved for  $A = \partial i \setminus j$ , yielding a computational cost  $\mathcal{O}(z^2 M^6)$  for the update of  $z$  messages.

For the SIS model we pick  $y_A^t$  to be the event that at least one of  $k \in A$  infects  $i$ :

$$p(y_k^t | x_k^t, x_i^t) = \begin{cases} \lambda_{ki} \delta(y_j^t, I) + (1 - \lambda_{ki}) \delta(y_k^t, S) & \text{if } x_k^t = S \\ \delta(y_k^t, S) & \text{otherwise} \end{cases} \quad (\text{E10})$$

$$p(y_{A \cup B}^t | y_A^t, y_B^t, x_i^t) = \delta(y_{A \cup B}^t, I) \mathbb{1}[y_A^t = I \vee y_B^t = I] + \delta(y_{A \cup B}^t, S) \mathbb{1}[y_A^t = S \wedge y_B^t = S]. \quad (\text{E11})$$

In this case, all  $y$  variables are binary, yielding a computational cost  $\mathcal{O}(zM^6)$  for the update of  $z$  messages.

## Appendix F: Discretized mean-field methods

We report the expressions for the discretized version of Individual-Based Mean Field (IBMF) and Dynamic Message Passing (DMP) which were used to produce the data in fig. 1. They consist in a discrete time evolution for the expectation of single-variable marginals and cavity marginals (only DMP). In the limit of infinitesimal time-step, they reduce to their continuous counterparts. Define  $I_i^t$  as the probability of individual  $i$  being in state  $I$  at time  $t$ ,  $I_{i \rightarrow j}^t$  ( $(ij) \in E$ ) the probability of individual  $i$  being in state  $I$  at time  $t$  and having been infected by someone other than  $j$ . We parametrize transmission and recovery probabilities as a rate  $\lambda, \rho$  times the time-step  $\Delta t$  so that in the continuous-time limit, the equations in their original version are recovered in terms of rates.

For IBMF we have

$$I_i^{t+\Delta t} = (1 - \rho_i \Delta t) I_i^t + \left( 1 - \prod_{j \in \partial i} (1 - \lambda_{ji} \Delta t I_j^t) \right) (1 - I_i^t) \quad (\text{F1})$$

and for DMP

$$I_i^{t+\Delta t} = (1 - \rho_i \Delta t) I_i^t + \left( 1 - \prod_{j \in \partial i} (1 - \lambda_{ji} \Delta t I_{j \rightarrow i}^t) \right) (1 - I_i^t) \quad (\text{F2})$$

$$I_{i \rightarrow j}^{t+\Delta t} = (1 - \rho_i \Delta t) I_{i \rightarrow j}^t + \left( 1 - \prod_{k \in \partial i \setminus j} (1 - \lambda_{ki} \Delta t I_{k \rightarrow i}^t) \right) (1 - I_{i \rightarrow j}^t) \quad (\text{F3})$$

## Appendix G: Exact mappings

We show examples of models which can be represented exactly by a MPS.

*a. Models with mass on a finite support* Any arbitrary distribution  $p(\bar{x}) = p(x^0, x^1, \dots, x^T)$  can in principle be represented via a MPS, albeit with matrix size exponentially large in  $T$ : to see this, re-write  $p$  trivially as a superposition of delta distributions

$$p(\bar{x}) = \sum_{\bar{y}} p(\bar{y}) \prod_{t=0}^T \delta(x^t, y^t) \quad (\text{G1})$$

where the product over  $t$  is interpreted as a product of  $1 \times 1$  matrices. Since the linear combination of two MPSs is itself a MPS:

$$a \prod_t A^t(x^t) + b \prod_t B^t(x^t) = \prod_t C^t(x^t) \quad (\text{G2})$$

with

$$C^0(x^0) = [a \ A^0(x^0) \ b \ B^0(x^0)], \quad C^t(x^t) = \begin{bmatrix} A^t(x^t) & 0 \\ 0 & B^t(x^t) \end{bmatrix}, \quad C^T(x^T) = \begin{bmatrix} A^T(x^T) \\ B^T(x^T) \end{bmatrix} \quad (\text{G3})$$

then  $p$  can be expressed by a MPS with matrix size  $q^T$ ,  $q$  being the number of values taken by each  $x^t$ . Now, if the distribution under consideration puts non-zero probability only over a small set  $\mathcal{T}$  of trajectories, the number of components in the superposition, and hence the final matrix size, is  $|\mathcal{T}|$ .

Any non-recurrent and Markovian model like SIR (Susceptible Infectious Recovered), SEIR (Susceptible Exposed Infectious Recovered), etc., allows only a sub-exponential fraction of the  $2^T$  potential trajectories. Take as an example the SIR model: each message  $m_{i \rightarrow j}$  can be parametrized by the infection and recovery times for individuals  $i$  and  $j$ , for a total  $\mathcal{O}(T^4)$  possible trajectories. The same reasoning goes for a generic non-recurrent Markovian model with  $q$  states, yielding matrix size  $\mathcal{O}(T^{q^2})$ .

*b. Chain models* Consider  $T + 1$  variables each taking one in  $q$  values whose distribution is factorized over an open chain

$$p(x^0, x^1, \dots, x^T) \propto \prod_{i=0}^{T-1} \psi^i(x^i, x^{i+1}). \quad (\text{G4})$$

We show that there exists an equivalent formulation in MPS form, with matrices of size  $q \times q$ . Introduce additional variables  $\{a^t\}_{t=1:T}$  with  $a^t = x^t$  to get

$$p(x^1, x^2, \dots, x^T) \propto \sum_{a^1, a^2, \dots, a^T} \delta(x^0, a^1) \prod_{t=0}^{T-2} \{ \psi^t(a^{t+1}, x^{t+1}) \delta(x^{t+1}, a^{t+2}) \} \psi^{T-1}(a^T, x^T) \quad (\text{G5})$$

$$\propto \sum_{a^1, a^2, \dots, a^T} [A^0(x^0)]_{a^1} \prod_{t=1}^{T-1} [A^t(x^t)]_{a^t, a^{t+1}} [A^T(x^T)]_{a^T} \quad (\text{G6})$$

$$\propto \prod_{t=0}^T A^t(x^t) \quad (\text{G7})$$

with

$$\begin{cases} [A^0(x^0)]_{a^1} &= \delta(x^0, a^1) \\ [A^t(x^t)]_{a^t, a^{t+1}} &= \psi^{t-1}(a^t, x^t) \delta(x^t, a^{t+1}) \quad \forall t \in 1, 2, \dots, T-1 \\ [A^N(x^T)]_{a^N} &= \psi^{T-1}(a^T, x^T) \end{cases} \quad (\text{G8})$$

where each  $a$  ranges over  $q$  values. We note the following implication: messages in the 1-step DMP method Del Ferraro and Aurell [3], which are parametrized as chain models, can be represented with matrices of size  $q^2 \times q^2$ .

*c. One-particle trajectories in the SI model* We show that the probability of any trajectory of an individual in the SI model can be represented by a MPS with matrices of size  $2 \times 2$ . It suffices to show that such probability factorizes over a chain. In the following we will sometimes use the convention  $S = 0, I = 1$ . The rule that once an individual  $i$  is infected at time  $t$  it can never recover is then encoded compactly as  $\prod_{t=1}^T \mathbb{1}[x_i^{t+1} \geq x_i^t]$ .

For a generic time  $t$  consider the conditional probability  $p(x^{t+1}|x^0, x^1, \dots, x^t)$ . If  $x^t = I$  then  $p(x^{t+1}|x^0, x^1, \dots, x^t) = \delta(x^{t+1}, I)$ . If  $x^t = S$  then it must also be that  $x^0 = x^1 = \dots = x^{t-1} = S$ . We conclude that the state at time  $t+1$  depends on the previous states only through the state at time  $t$ :  $p(x^{t+1}|x^0, x^1, \dots, x^t) = p(x^{t+1}|x^t)$ . Hence,

$$p(x^0, x^1, \dots, x^N) = \prod_{t=0}^{T-1} p(x^{t+1}|x^0, x^1, \dots, x^t) = \prod_{t=0}^{T-1} p(x^{t+1}|x^t) \quad (\text{G9})$$

The same thesis can be proven via a different argument: for “non-recurrent” models like SI, information about the trajectory can be encoded into a single parameter: the infection time. Infection at some time  $t_i \in \{0, 1, \dots, T, \infty\}$  (we use the convention that no infection corresponds to  $t = \infty$ ) corresponds to  $x^0 = \dots = x^{t-1} = S, x^t = \dots, x^T = I$ . It is sometimes convenient to switch between these two equivalent representations.

We propose a chain-factorized ansatz and show that it fully specifies the probability of a trajectory

$$p(x^0, x^1, \dots, x^T) = \left[ \prod_{t=0}^{T-1} \mathbb{1}[x^t \leq x^{t+1}] q^t(x^t) \right] q^T(x^T). \quad (\text{G10})$$

The probability of any of the allowed trajectories is

$$p(t_i = t) = p(x^0 = \dots = x^{t-1} = S, x^t = \dots, x^T = I) = \prod_{t=0}^{t-1} q^t(S) \prod_{t=t}^T q^t(I). \quad (\text{G11})$$

The ratio of probabilities of infection at times  $t+1$  and  $t$  gives

$$\frac{p(t_i = t+1)}{p(t_i = t)} = \frac{q^t(S)}{q^t(I)}. \quad (\text{G12})$$

Parametrizing as  $q^t(S) \propto 1, q^t(I) \propto e^{-h^t}$ , we get

$$h^t = \log \frac{q^t(S)}{q^t(I)} = \log \frac{p(t_i = t+1)}{p(t_i = t)}. \quad (\text{G13})$$

In full detail, the resulting MPS is

$$\begin{cases} [A^0(x^0)]_{a^1} & = \delta(x^0, a^1) \\ [A^t(x^t)]_{a^t, a^{t+1}} & = \mathbb{1}[a^t \leq x^t] q^{t-1}(a^t) \delta(x^t, a^{t+1}) \quad \forall t \in 1, \dots, T-1 \\ [A^T(x^T)]_{a^T} & = \mathbb{1}[a^T \leq x^T] q^{T-1}(a^T) q^T(x^T) \end{cases} \quad (\text{G14})$$

*d. Pair trajectories in the SI model* We show that any BP message in the SI model can be represented exactly by a MPS with matrices of size  $6 \times 6$ . Consider the BP equations for the SI model parametrized with infection times (see Altarelli *et al.* [35])

$$m_{i \rightarrow j}(t_i, t_j) \propto \sum_{t_{\partial i \setminus j}} \delta\left(t_i, \min_{k \in \partial i} \{t_k\}\right) \prod_{k \in \partial i \setminus j} m_{k \rightarrow i}(t_k, t_i) \quad (\text{G15})$$

$$\propto \mathbb{1}[t_i \leq t_j] \prod_{k \in \partial i \setminus j} \sum_{t_k} \mathbb{1}[t_i \leq t_k] m_{k \rightarrow i}(t_k, t_i) - \mathbb{1}[t_i < t_j] \prod_{k \in \partial i \setminus j} \sum_{t_k} \mathbb{1}[t_i < t_k] m_{k \rightarrow i}(t_k, t_i) \quad (\text{G16})$$

$$\propto \mathbb{1}[t_i \leq t_j] a_{i \rightarrow j}(t_i) - \mathbb{1}[t_i < t_j] b_{i \rightarrow j}(t_i) \quad (\text{G17})$$

$$\propto \mathbb{1}[t_i \leq t_j] c_{i \rightarrow j}(t_i) + \mathbb{1}[t_i = t_j] b_{i \rightarrow j}(t_i) \quad (\text{G18})$$

where we used  $\delta(x, \min_{k \in S} \{x_k\}) = \prod_{k \in S} \mathbb{1}[x \leq x_k] - \prod_{k \in S} \mathbb{1}[x < x_k]$  and defined  $a_{i \rightarrow j}(t_i) = \prod_{k \in \partial i \setminus j} \sum_{t_k} \mathbb{1}[t_i \leq t_k] m_{k \rightarrow i}(t_k, t_i)$ ,  $b_{i \rightarrow j}(t_i) = \prod_{k \in \partial i \setminus j} \sum_{t_k} \mathbb{1}[t_i < t_k] m_{k \rightarrow i}(t_k, t_i)$ ,  $c_{i \rightarrow j}(t_i) = a_{i \rightarrow j}(t_i) - b_{i \rightarrow j}(t_i)$ .

Once normalized, both  $c_{i \rightarrow j}$  and  $b_{i \rightarrow j}$  are probability distributions for a single SI trajectory, hence they can be re-parametrized (with a slight abuse of notation) as MPSs  $c_{i \rightarrow j}(x_i) = \prod_t \mathbb{1}[x_i^{t+1} \geq x_i^t] \tilde{c}_{i \rightarrow j}^t(x_i)$ ,  $b_{i \rightarrow j}(x_i) = \prod_t \mathbb{1}[x_i^{t+1} \geq x_i^t] \tilde{b}_{i \rightarrow j}^t(x_i)$ . Introducing the SI rule also for  $x_j$ , we get

$$m_{i \rightarrow j}(x_i, x_j) \propto \prod_t \mathbb{1}[x_i^t = x_j^t] \mathbb{1}[x_i^{t+1} \geq x_i^t] \tilde{b}_{i \rightarrow j}(x_i) + \prod_t \mathbb{1}[x_i^t \leq x_j^t] \mathbb{1}[x_i^{t+1} \geq x_i^t] \mathbb{1}[x_j^{t+1} \geq x_j^t] \tilde{c}_{i \rightarrow j}^t(x_i). \quad (\text{G19})$$

The first term is a chain-factorized distribution for, say,  $x_i$  times the constraint  $x_j^t = x_i^t \forall t$ , hence it can be represented as an MPS with  $2 \times 2$  matrices. The second term is a chain of 4-state variables  $\{(x_i^t, x_j^t)\}_{t=0:T}$ , hence it can be represented as an MPS with  $4 \times 4$  matrices. In full detail

$$\prod_t \mathbb{1}[x_i^t = x_j^t] \mathbb{1}[x_i^{t+1} \geq x_i^t] \tilde{b}_{i \rightarrow j}(x_i) = \sum_{a_i^1, \dots, a_i^T} \prod_t \underbrace{\mathbb{1}[x_i^t = x_j^t] \delta(x_i^t, a_i^{t+1})}_{[B^t(x_i^t, x_j^t)]_{a_i^t, a_i^{t+1}}} \mathbb{1}[a_i^t \leq x_i^t] b_{i \rightarrow j}^{t-1}(a_i^t) \quad (\text{G20})$$

$$\prod_t \mathbb{1}[x_i^t \leq x_j^t] \mathbb{1}[x_i^{t+1} \geq x_i^t] \mathbb{1}[x_j^{t+1} \geq x_j^t] \tilde{c}_{i \rightarrow j}^t(x_i) = \sum_{\substack{a_i^1, \dots, a_i^T \\ a_j^1, \dots, a_j^T}} \prod_t \underbrace{\mathbb{1}[x_i^t \leq x_j^t] \delta(x_i^t, a_i^{t+1}) \delta(x_j^t, a_j^{t+1})}_{[C^t(x^t)]_{(a_i^t, a_j^t), (a_i^{t+1}, a_j^{t+1})}} \mathbb{1}[a_i^t \leq x_i^t] \mathbb{1}[a_j^t \leq x_j^t] \tilde{c}_{i \rightarrow j}^{t-1}(a_i^t) \quad (\text{G21})$$

Finally, since the mixture of two MPSs is itself an MPS (G2), we get that  $m_{i \rightarrow j}$  can be written as a MPS with matrices of size  $2 + 4 = 6$ .

## Appendix H: Pair-wise reweightings

The distribution 2 can be made more general by adding reweighting terms involving neighboring variables  $\{\psi_{ij}^t(x_i^t, x_j^t)\}_{(ij) \in E}$ . Now

$$p(\bar{x}) \propto \prod_{i=1}^N w(x_i^0) \prod_{t=0}^{T-1} \prod_{i=1}^N w(x_i^t | x_{\partial i}^{t-1}, x_i^{t-1}) \phi_i^t(x_i^t) \prod_{(ij)} \psi_{ij}^t(x_i^t, x_j^t) \quad . \quad (\text{H1})$$

The message ansatz stays the same. The BP equation becomes

$$m_{i \rightarrow j}(\bar{x}_i, \bar{x}_j) \propto \sum_{\bar{x}_{\partial i \setminus j}} w(x_i^0) \phi_i^0(x_i^0) \prod_t w(x_i^{t+1} | \mathbf{x}_{\partial i}^t, x_i^t) \phi_i^{t+1}(x_i^{t+1}) \prod_{k \in \partial i \setminus j} \psi_{ik}^{t+1}(x_i^{t+1}, x_k^{t+1}) \prod_{k \in \partial i \setminus j} m_{k \rightarrow i}(\bar{x}_k, \bar{x}_i) \quad (\text{H2})$$

and the  $B$  matrices read

$$\begin{aligned} [B_{i \rightarrow j}^0(x_i^1, x_i^0, x_j^0)]_{\{a_k^1\}_{k \in \partial i \setminus j}} &= w(x_i^0) \phi_i^0(x_i^0) \sum_{\{x_k^0\}_{k \in \partial i \setminus j}} w(x_i^1 | \mathbf{x}_{\partial i}^0, x_i^0) \prod_{k \in \partial i \setminus j} \psi_{ij}^0(x_k^0, x_i^0) [A_{k \rightarrow i}^0(x_k^0, x_i^0)]_{a_k^1} \\ [B_{i \rightarrow j}^t(x_i^{t+1}, x_i^t, x_j^t)]_{\{a_k^t, a_{k+1}^t\}_{k \in \partial i \setminus j}} &= \phi_i^t(x_i^t) \sum_{\{x_k^t\}_{k \in \partial i \setminus j}} w(x_i^{t+1} | \mathbf{x}_{\partial i}^t, x_i^t) \prod_{k \in \partial i \setminus j} \psi_{ik}^t(x_k^t, x_i^t) [A_{i \rightarrow j}^t(x_i^t, x_j^t)]_{a_k^t, a_{k+1}^{t+1}} \quad (\text{H3}) \\ &\quad \forall t \in \{1, \dots, T-1\} \\ [B_{i \rightarrow j}^T(x_i^T, x_j^T)]_{\{a_k^T\}_{k \in \partial i \setminus j}} &= \phi_i^T(x_i^T) \sum_{\{x_k^T\}_{k \in \partial i \setminus j}} \prod_{k \in \partial i \setminus j} \psi_{ik}^T(x_i^T, x_k^T) [A_{k \rightarrow i}^T(x_k^T, x_i^T)]_{a_k^T}. \end{aligned}$$